Magazine of Civil Engineering

ISSN 2712-8172

journal homepage: http://engstroy.spbstu.ru/

Research article

UDC 666.9.03

DOI: 10.34910/MCE.111.15

3D-printable artificial marble

G.S. Slavcheva ✉, ***E.A. Britvina***
Voronezh State Technical University, Voronezh, Russia
✉ *gslavcheva@yandex.ru*

Keywords: additive manufacturing, 3d-printable material, rheological behavior, compressive strength, setting time

Abstract. This paper presents the rheological and hardened properties of novel 3D-printable materials imitating structures of marble. The effects of mixed proportion on rheological behavior, kind of texture, setting time, density, compressive strength, water absorption, drying shrinkage, frost resistance are presented together. Two kinds of squeezing tests were used to evaluate the extrusion ability and shape stability of the fresh mixture. A high compression speed test using constant plate speed of 5 mm/s was implemented to simulate the behavior of the system in the process of extrusion. The squeezing test was conducted with a constant strain rate of 0.5 N/s as to model the behavior of the system in the process of multi-layer casting. Properties of the 3D-printable artificial marble were determined by Russian standards. The fresh mixtures of 3D-printable artificial marbles had plastic yield value of 1.2–3.5 kPa, structural strength of 1.2–3.3 kPa, the value of plastic deformations was 0.05–0.06 mm/mm. This defined the ability of these mixtures to plastically deform without structure destruction and hold their form, resist the deformation under compressions load during multi-layer casting. The received specimens of artificial marble resemble six kinds of textures of white and color marble. The 3D-printable artificial marble had high compressive strength (36–48 MPa and 55–68 MPa at 1 day and 28 days after production respectively), low water absorption (0.75 %), drying shrinkage (1.3–1.9 mm/m), high frost resistance and short setting time that determine the effectiveness of 3D-printed structures life cycle.

1. Introduction

The idea of scaling up additive manufacturing techniques for automated building construction has been a topic of research for several years [1–8]. Research to date can be classified into the next groups:

- pumpability, extrusion ability, printability, buildability, open time of 3D-printable mixture [9–14];
- component design, properties, and durability of 3D-printed composite materials [15–19];
- modeling, mechanics, and control of the 3D-printing process [10, 11, 20–22];
- demonstrating the viability of 3D-printed structures [23–26].

According to review [18, 19], the component design is the interdependent factor affecting mechanics and control of the 3D-printing process and viability of 3D-printed structures. The material is typically a high cement content mortar, which contents a different kind of aggregates with a maximum particle size in the order of 2 mm to 3 mm, plasticizer, viscosity modifying additive, fiber.

At the same time, the typical viable 3D-printed structures are printed shells watch that have a function of permanent formwork. All known and used compositions of 3D-printed materials are produced by using grey cement and plain, monochrome aggregates. As a result, 3D-printed structures are grey and plain too and need finishing and painting in order to provide their architectural expressiveness. It is obvious that the

finishing requires a lot of handwork that would discredit the idea of robotic 3D-printing technology. The solution to this problem can be the usage of decorative concrete, whose properties would be adapted to the printing process.

However, all known kind of color decorative concretes are used in traditional concrete casting technology [27–30]. Therefore, the development of 3D-printable decorative concrete would allow the 3D-printed structures to obtain architectural expressiveness without additional costs for their finishing.

This paper aims to contribute to this promising line of research, and reports on outcomes of a research program aimed to develop a novel 3D-printable decorative concrete.

2. Materials and Methods

Six types of 3D-printable cement pastes were studied (Table 1). The initial components were used of the system:

- white Portland cement CEM I 52.5 R (EN 197 – 1: 2011),
- the plasticizer of Sika trademark based on polycarboxylate ethers,
- complex viscosity modifying additive,
- three kinds of aggregates, limestone filler ($CaCO_3$ content ~ 95%; a particle size distribution ranging from 1 to 75 μm),
- polypropylene fiber (l = 12 mm, d = 0.022 – 0.034 mm),
- pigments (Fe_2O_3 content ~ 80%).

Table 1. Tested cement paste composition and specimen identification.

Specimen ID	Components/ mass cement (%)						W/C	kind of aggregates
	plasticizer	complex viscosity modifying additive	polypropylene fiber	aggregates	limestone filler	pigment		
T1	1.2	0.4	0.5	125	-	-	0.32	sand
T2	1.2	0.4	0.5	125	-	-	0.35	granite
T3	1.2	0.4	0.5	100	25	-	0.39	slate
T4	1.2	0.4	0.5	125	-	0.2 (red)	0.35	granite + slate
T5	1.2	0.4	0.5	125	-	0.2 (green)	0.35	granite + serpentine
T6	1.2	0.4	0.5	100	25	-	0.38	granite + slate

The aggregates had a particle size distribution ranging from 0 to 5 mm (Table 2). The white Portland cement and aggregates with different colors and particle sizes have been used to achieve the imitation structure of marble. W/C- ratio, concentration, and the particle size range of aggregates, the concentration of limestone filler was assumed as the main factors for the change of rheological behaviour of the 3D-printable cement pastes. Content of plasticizer, complex viscosity modifying additives, polypropylene fiber were assumed as a fixed factor for the experiments.

Table 2. The particle size distribution of limestone filler.

kind of aggregates	color	particle size range	
		volume of particles, %	size (d), μm
sand	white	13.2	630
		49.3	315
		37.5	160
granite	yellow	67.0	
		13.0	1250
		20.0	630
slate	terracotta	~ 98	2500
serpentine	green	65.4	5000
		34.6	2500

To evaluate the extrusion ability and firm stability of fresh mixture, the different kinds of squeezing tests were used following the methodology developed in the works [10, 20–22, 31, 32].

Cylindrical samples of fresh cement paste with radius R equal to their height h_0 = 25 mm were used for the implementation of the experiment. For the squeezing test, the sample was put between two smooth plates diameter of which corresponded to the size of the sample and was loaded into the testing system "INSTRON Sates 1500 HDS". The test was conducted on a fresh sample for all mixtures directly after their molding.

High compression speed test using constant plate speed ν = 5 mm/s was implemented as the behaviour of the system in the process of extrusion is most adequately modeled with this speed. The curves "compression force N is displacement Δ_{pl}" were obtained during the experiments were interpreted as influence curves of reduced compression load F^* from a relative change of height of the sample h_i/R:

$$F_i^* = \frac{Ph_i}{\pi R^2}, \quad (1)$$

where $h_i = (h_0 - \Delta)$, h_0 is the initial height of the sample, Δ is transferred in the point of time, value R was taken as constant and equal to the radius of the sample at the beginning of the experiment.

According to the results of the analysis of the received experimental curves for the studied system's values K_i, called plastic yield value by N. Roussel and C. Lanos [20, 21], was calculated at the inflection point of the $F^*(h_i/R)$ curves $(h_i/R = 0.9)$:

$$K_i\left(h_i/R\right) = \frac{\sqrt{3}F^*}{2} \quad (2)$$

The squeezing test was conducted with a constant strain rate ν = 0.5 N/s was implemented as the behaviour of the system in the process of multi-layer casting [32]. The strain rate conforms to the average speed of load increase during multi-layer casting of building sites by industrial printers. The methodology of its implementation corresponds to the approaches of A. Perrot [10, 22] to the evaluation of the buildability of the 3D printable mixtures. Squeezing was conducted until the rupture of the samples. The curves "displacement Δ_{pl} – time τ", "displacement Δ is compression force N" were recorded as the result of the experiments. Based on the obtained experimental curves, structural strength (σ_0) of fresh mixtures was calculated for the moments corresponding to the start of deformation (Δ_{pl} = 0.1 mm), and plastic strength (σ_{pl}) was calculated at the beginning of cracking. The value of plastic deformations Δ_{pl} at the start of cracking was determined as a ratio of the displacement Δ of the plates in the squeezing test to the initial height of the sample h_0.

Properties of the 3D-printable artificial marble were determined by Russian standards:

- water absorption according to Russian State Standard GOST 12730.3 "Concretes. Method of determination of water absorption";

- setting time according to Vicat method (Russian State Standard GOST 310.3 "Cements. Methods for determination of standard consistency, times of setting and soundness");

- compressive strength according to Russian State Standard GOST 10180 – 12 "Concretes. Methods for strength determination using reference specimens" using the universal 4-column static hydraulic testing system "INSTRON Sates 1500 HDS",

- frost resistance according to Russian State Standard GOST 10060-2012 "Concretes. Methods for determination of frost-resistance" (the first basic method for repeated freezing and thawing),

- drying shrinkage according to Russian State Standard GOST 24544-2020 "Concretes. Methods of shrinkage and creep flow determination".

3. Results and Discussion

3.1. Rheological behaviour

The rheological properties of fresh mixtures for 3D-printable artificial marble are listed in Table 3. Results of two kind of squeezing tests are shown in Figure 1, 2.

Table 3. Rheological properties of 3D-printable artificial mixtures.

Specimen ID	Plastic yield value K_i, kPa	Strength, kPa		Value of plastic deformations Δ_{pl}, mm/mm
		structural σ_0	plastic σ_{pl}	
T1	2.38	0.74	45.78	0.06
T2	1.23	1.42	42.25	0.08
T3	4.70	0.41	51.41	0.06
T4	3.49	1.95	40.71	0.05
T5	1.72	3.29	35.13	0.05
T6	2.35	1.19	28.54	0.06

As a result of the interpretation of the squeezing test with constant plate speed, we received experimental curves $F^* = f(h_i/R)$ (Fig. 1) which correspond to the similar curves of N. Roussel [21]. Analysis of experimental curves $F^* = f(h_i/R)$ for the description of rheological behavior of fresh artificial marble paste during squeezing was conducted based on approaches of fundamental structural rheology of disperse systems [31].

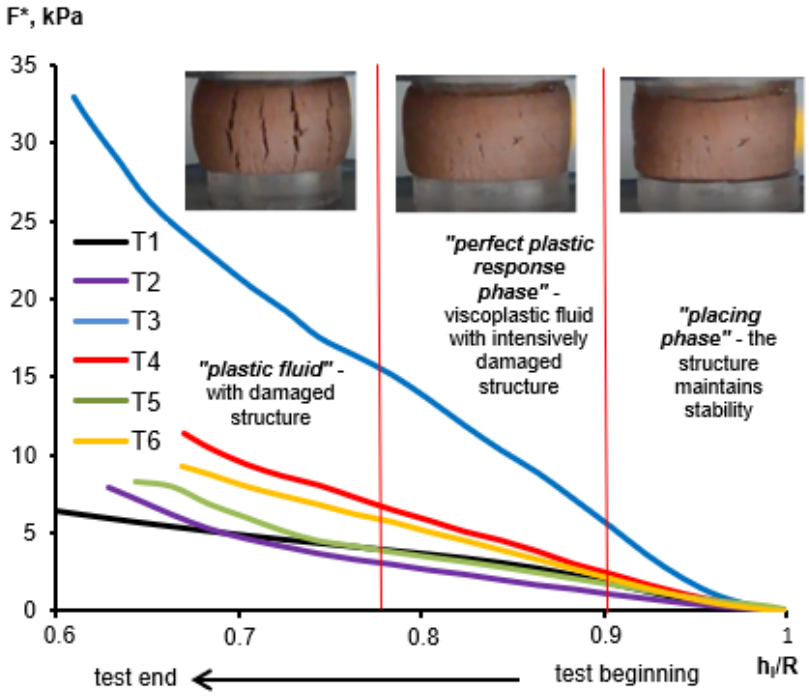

Figure 1. Tested artificial marble *F*(hi/R)* curves.

Under the action of low compression stress on the first section of the curve within deformation range ~ 0.9 < h_i/R < 1 the structure maintains stability ("placing phase" according to N. Roussel's terminology). According to point of view structural rheology of disperse systems, the "placing phase" can be characterized as a viscoplastic fluid with undisturbed structure. When the stress on the second section increases with 0.8 < h_i/R < 0.9, the system is plastically deformed while its structure loses its stability ("perfect plastic response phase" according to N. Roussel). This section can be correlated with a viscoplastic fluid with intensively damaged structure in conformity with the structural rheology approach.

The experimental results show similar kinds of $F^*(h_i/R)$ curves for 5 studied systems (T1, T2, T4, T5, T6). They have expressed a horizontal section of plastic deformation. For the systems transfer from stable condition to plastic flow is estimated by load F^* for ~ 2.0 ÷ 3.0 kPa, transfer into the condition of the flow with damaged structure happens with F^* > 5.0 kPa. These mixtures can be extruded through an extruder nozzle with low squeezing force. The system T3 does not have the horizontal section of plastic deformation, transfer from stable condition to plastic flow is estimated by load F^* for ~ 6.0 kPa.

The systems T1, T2, T4, T5, T6 have rational values plastic yield value K_i = 1.2 -3.5 kPa (Table 3), which is determined at the beginning of the viscoplastic fluid of disperse system with undisturbed structure.

These values K_i ensure the best extrability due to their sufficient plasticity and capacity for viscoplastic flow without the structure damage under the influence of extrusion stress [32]. At the same time, the system T3 having the highest plastic yield value (K_i = 4.5 kPa) can not have a capacity for viscoplastic flow in the extrusion process due to high rigidity.

Analysis of the received experimental data of the curves "displacement Δ – time τ", "displacement Δ – compression force N" (Fig. 2) shows three typical zones of rheological behavior.

The first one is the zone of phase stability. The structural strength σ_0 is calculated based on the quantity load N at the beginning of deformation of viscoplastic mixtures can be considered as the main criterion of their buildability. The structural strength σ_0 characterizes the ability of the system to maintain stability without deformation during loading. The second one is the zone of the plastic phase. The system's ability to deform without destruction is evaluated by the quantity of plastic strength σ_{pl} calculated based on the quantity load N at the beginning of cracking. To characterize buildability, it seems reasonable to evaluate the number of plastic deformations on this section Δ_{pl}, which have to be minimized for 3D printable materials. The third one is the cracking phase and intensively destruction of the structure. The curves "$\Delta - \tau$" shows that all studied system displays the similar phase stability and plastic phase zone. However, the structural strength for system T3 is less in ~2 – 3 times comparing with the systems T1, T2, T4, T5, T6 (see Table 3).

a)

b)

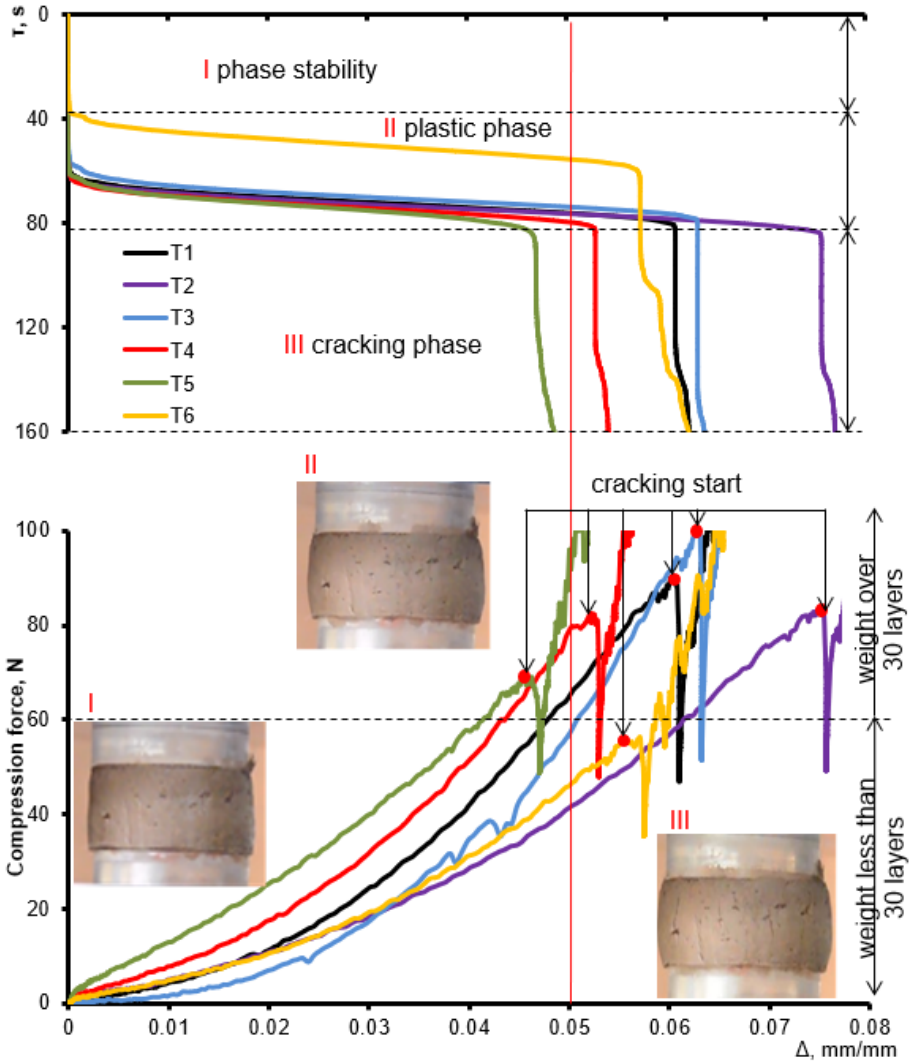

Figure 2. Tested artificial marble "displacement Δ – time τ" (a) and "displacement Δ – compression force N" (b) experimental results.

The transition between plastic yield value K_i, the value of structural σ_0 and plastic σ_{pl} strength, plastic deformations Δ_{pl} is linked to the concentration and a particle size distribution of the aggregates and filler. At the same time, the inclusion of pigments does not have a significant influence on the rheological properties of mixtures.

Change of rheological characteristics of mixture depends on kind of distribution of particle size. If aggregates have different particle sizes, their particles rationally locate between cement particles. As a result, dense spatial packing of solid particles into cement paste structure is ensured. Such structuring of the mixture solid-phase ensures the increase of their firm stability and consequently buildability. By contrast, aggregates having equal particle size loosen fresh mixture structure. This effect of decreasing plasticity and firm stability of mixtures is logically related to the influence of aggregates. Introduction of aggregates into dispersing system "cement + water" as a regulating factor of solid-phase properties changes packing density and molecular interactions between solid particles. As a result, flow under stress becomes difficult for coarser systems containing aggregates. For systems T1, T2, T4, T5, T6 (aggregates with different particle sizes (see Table 2)) plastic yield value K_i, corresponding to the beginning of the plastic flow, is in the range from 1.23 to 2.49 kPa. At the same time, these systems have enough firm stability (σ_0 = 1.2 – 3.3 kPa, Δ_{pl} = 0.05 – 0.06). The system T3 (aggregates with equal particle size) is characterized by the highest rigidity (K_i = 4.70 kPa) and the least firm stability (σ_0 = 0.41 kPa, Δ_{pl} = 0.06). Therefore, usage of aggregates with different particle sizes allows the fresh mixture to obtain plasticity and firm stability but usage of aggregates with equal particle size would not be possible to ensure that.

3.2. Properties of 3D-printable artificial marble

As shown in Figure 3, all the specimens of received 3D-printable composites resemble the structures of marble. System T1 imitates the structure of white marble; the systems T2 – T6 imitate the different structures of color marble.

Table 4 shows the properties of specimens of received 3D-printable artificial marble. The average density of all the specimens is 2150 kg/m^3, the average water absorption is 0.75 %, frost resistance 200 cycles, drying shrinkage 1.3–1.9 mm/m. The compressive strength of 3D-printable artificial marble specimens is in the range from 36.5 to 47.7 MPa at 1 day after production; from 54.5 to 67.9 MPa at 28 days after production. In 1 day of hardening 3D-printable artificial marble occurs the most intensive growth of the strength. It is important to emphasize that in this period the strength receives 75 -80 % from 28 days strength.

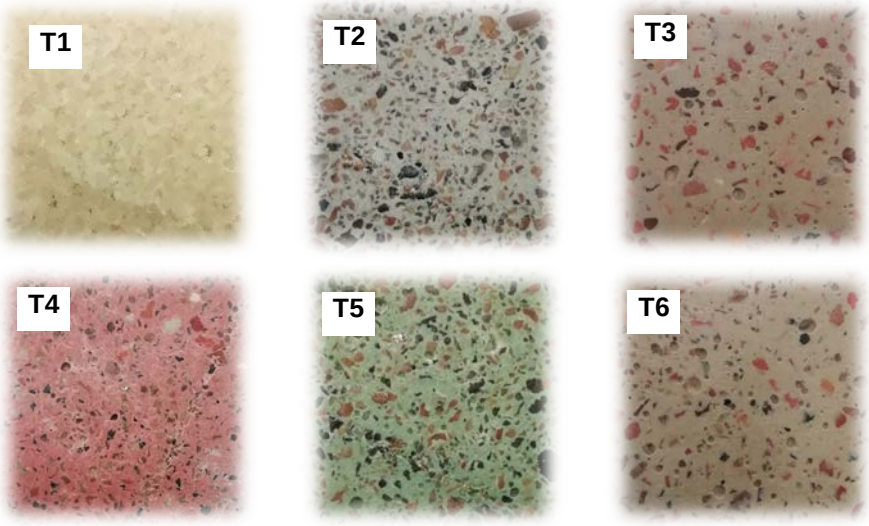

Figure 3. The structures of 3D-printable artificial marble.

Table 4. Properties of 3D-printable artificial marble.

Specimen ID	Density, kg/m^3	Water absorption, %	Setting time, min	Compressive strength, MPa		Frost resistance, cycle	Drying shrinkage, mm/m
				1 day	28 days		
T1	2250	0.2	105	47.7	67.9	200	≤ 1.6
T2	2200	0.3	105	44.8	60.9	200	≤ 1.4
T3	2150	1.7	120	47.5	66.6	200	≤ 1.7
T4	2250	0.8	75	41.6	63.8	200	≤ 1.4
T5	2150	0.9	60	36.5	54.5	200	≤ 1.3
T6	2150	0.6	120	42.2	63.6	200	≤ 1.9

These results indicate that changing the kind of aggregates, the inclusion of pigments does not have a significant influence on the properties of materials. On the other hand, the inclusion of pigments has a positive influence on the setting time of mixtures. The systems without pigments (T1, T2, T3, T6) are characterized by setting time 105–120 min, the systems with pigments (T4, T5) are characterized by setting time 60–75 min. That is due to the pigment content directly related to the hydration process despite the aggregates kind and ratio varies.

The high early-age strength, short setting time, low water absorption and drying shrinkage, high frost resistance are very impotent attributes to 3D-printable materials because they determine the effectiveness of building technology and durability of 3D-printed structures.

4. Conclusion

Six kinds of structures of 3D-printable artificial marbles have been received using white Portland cement, pigments, and aggregates with different colors and particle sizes.

The fresh mixtures of 3D-printable artificial marbles had plastic yield value $K_i \cong 1.2 – 3.5$ kPa that is defined the ability of these mixtures to plastically deform without structure destruction and maintain stability during extrusion. At the same time, these systems had enough firm stability (structural strength σ_0 = 1.2 – 3.3 kPa, the value of plastic deformations Δ_{pl} = 0.05– 0.06 mm/mm) that is characterized the system's ability to hold its form, resist the deformation under compressions load during multi-layer casting.

The optimal rheological characteristics of fresh mixtures can be achieved with the usage of aggregates with different particle sizes. The fresh mixtures having aggregate's particle size range from 0.15 to 5 mm are characterized by the optimal plasticity, structural strength, and deformability under the load. Using aggregates with equal particle size impairs these characteristics of mixtures.

The 3D-printable artificial marble had high compressive strength (36–48 MPa and 55–68 MPa at 1 day and 28 days after production respectively), low water absorption (0.75 %) and drying shrinkage (1.3–1.9 mm/m), high frost resistance and short setting time that determine the effectiveness of 3D-printed structures life cycle.

5. Acknowledgments

The experimental studies have been carried out using the facilities of the Collective Research Center named after Professor Yu.M. Borisov, Voronezh State Technical University, which is partly supported by the Ministry of Science and Education of the Russian Federation, Project No 075- 15-2021-662

References

1. Lim, S., Buswell, R.A., Le, T.T., Austin, S.A., Gibb, A.G.F., Thorpe, T. Developments in construction-scale additive manufacturing processes. Automation in Construction. 2012. 21(1). Pp. 262–268. DOI:10.1016/j.autcon.2011.06.010
2. Zhang, J., Wang, J., Dong, S., Yu, X., Han, B. A review of the current progress and application of 3D printed concrete. Composites Part A: Applied Science and Manufacturing. 2019. 125. Pp. 105533. DOI:10.1016/j.compositesa.2019.105533
3. Labonnote, N., Rønnquist, A., Manum, B., Rüther, P. Additive construction: State-of-the-art, challenges and opportunities. Automation in Construction. 2016. 72. Pp. 347–366. DOI:10.1016/j.autcon.2016.08.026
4. Buswell, R.A., Leal de Silva, W.R., Jones, S.Z., Dirrenberger, J. 3D printing using concrete extrusion: A roadmap for research. Cement and Concrete Research. 2018. 112. Pp. 37–49. DOI:10.1016/j.cemconres.2018.05.006
5. Ngo, T.D., Kashani, A., Imbalzano, G., Nguyen, K.T.Q., Hui, D. Additive manufacturing (3D printing): A review of materials, methods, applications and challenges. Composites Part B: Engineering. 2018. 143. Pp. 172–196. DOI: https://doi.org/10.1016/j.compositesb.2018.02.012.
6. Shakor, P., Nejadi, S., Paul, G., Malek, S. Review of emerging additive manufacturing technologies in 3d printing of cementitious materials in the construction industry. Frontiers in Built Environment. 2019. 4(85). Pp. 1–17. DOI:10.3389/fbuil.2018.00085
7. Wangler, T., Roussel, N., Bos, F.P., Salet, T.A.M., Flatt, R.J. Digital Concrete: A Review. Cement and Concrete Research. 2019. 123. Pp. 105780. DOI: https://doi.org/10.1016/j.cemconres.2019.105780
8. Khan, M.S., Sanchez, F., Zhou, H. 3-D printing of concrete: Beyond horizons. Cement and Concrete Research. 2020. 133. Pp. 106070. DOI: 10.1016/j.cemconres.2020.106070
9. Liu, Z., Li, M., Weng, Y., Wong, T.N., Tan, M.J. Mixture Design Approach to optimize the rheological properties of the material used in 3D cementitious material printing. Construction and Building Materials. 2019. 198. Pp. 245–255. DOI: 10.1016/j.conbuildmat.2018.11.252
10. Perrot, A., Rangeard, D., Pierre, A. Structural built-up of cement-based materials used for 3D-printing extrusion techniques. Materials and Structures/Materiaux et Constructions. 2016. 49. Pp. 1213–1220. DOI: 10.1617/s11527-015-0571-0
11. Roussel, N. Steady and transient flow behaviour of fresh cement pastes. Cement and Concrete Research. 2005. 35. Pp. 1656–1664. DOI: 10.1016/j.cemconres.2004.08.001
12. Nerella, V.N., Näther, M., Iqbal, A., Butler, M., Mechtcherine, V. Inline quantification of extrudability of cementitious materials for digital construction. Cement and Concrete Composites. 2019. 95. Pp. 260–270. DOI: 10.1016/j.cemconcomp.2018.09.015
13. Charrier, M., Ouellet-Plamondon, C. Testing Procedures on Materials to Formulate the Ink for 3D Printing. Transportation Research Record. 2020. 2674(2). DOI: 10.1177/0361198120907583

14. Le, T.T., Austin, S.A., Lim, S., Buswell, R.A., Gibb, A.G.F., Thorpe, T. Mix design and fresh properties for high-performance printing concrete. Materials and Structures/Materiaux et Constructions. 2012. 45(8). Pp. 1221–1232. DOI: 10.1617/s11527-012-9828-z
15. Le, T.T., Austin, S.A., Lim, S., Buswell, R.A., Law, R., Gibb, A.G.F., Thorpe, T. Hardened properties of high-performance printing concrete. Cement and Concrete Research. 2012. 42(3). Pp. 558–566. DOI: 10.1016/j.cemconres.2011.12.003
16. Feng, P., Meng, X., Chen, J.F., Ye, L. Mechanical properties of structures 3D printed with cementitious powders. Construction and Building Materials. 2015. 93. Pp. 486–497. DOI: 10.1016/j.conbuildmat.2015.05.132
17. Ma, G., Wang, L. A critical review of preparation design and workability measurement of concrete material for largescale 3D printing. Frontiers of Structural and Civil Engineering. 2018. 12(3). Pp. 382–400. DOI: 10.1007/s11709-017-0430-x
18. N.I. Vatin, L.I. Chumadova, I.S. Goncharov, V.V. Zykova, A.N. Karpenya, A.A. Kim, E.A. Finashenkov. 3D-Pechat V Stroitelstve. Stroitelstvo Unikalnykh Zdaniy I Sooruzheniy. 2017. 1(52). Pp. 27–46. DOI: 10.18720/CUBS.52.3
19. Lu, B., Weng, Y., Li, M., Qian, Y., Leong, K.F., Tan, M.J., Qian, S. A systematical review of 3D printable cementitious materials. Construction and Building Materials. 2019. 207. Pp. 477–490. DOI: 10.1016/j.conbuildmat.2019.02.144
20. Roussel, N., Lanos, C. Plastic fluid flow parameters identification using a simple squeezing test. Applied Rheology. 2003. 13(3). Pp. 132–141. DOI: 10.1515/arh-2003-0009
21. Toutou, Z., Roussel, N., Lanos, C. The squeezing test: A tool to identify firm cement-based material's rheological behaviour and evaluate their extrusion ability. Cement and Concrete Research. 2005. 35(10). Pp. 1891–1899. DOI: 10.1016/j.cemconres.2004.09.007
22. Perrot, A., Mélinge, Y., Rangeard, D., Micaelli, F., Estellé, P., Lanos, C. Use of ram extruder as a combined rheo-tribometer to study the behaviour of high yield stress fluids at low strain rate. Rheologica Acta. 2012. 51(8). Pp. 743–754. DOI: 10.1007/s00397-012-0638-6
23. Buswell, R.A., Soar, R.C., Gibb, A.G.F., Thorpe, A. Freeform Construction: Mega-scale Rapid Manufacturing for construction. Automation in Construction. 2007. 16. Pp. 224–231. DOI: 10.1016/j.autcon.2006.05.002
24. Khoshnevis, B. Automated construction by contour crafting - Related robotics and information technologies. Automation in Construction. 2004. Pp. 5–19. DOI: 10.1016/j.autcon.2003.08.012
25. Cesaretti, G., Dini, E., De Kestelier, X., Colla, V., Pambaguian, L. Building components for an outpost on the Lunar soil by means of a novel 3D printing technology. Acta Astronautica. 2014. 93. Pp. 430–450. DOI: 10.1016/j.actaastro.2013.07.034
26. Gosselin, C., Duballet, R., Roux, P., Gaudillière, N., Dirrenberger, J., Morel, P. Large-scale 3D printing of ultra-high performance concrete - a new processing route for architects and builders. Materials and Design. 2016. 100. Pp. 102–109. DOI: 10.1016/j.matdes.2016.03.097
27. López, A., Guzmán, G.A., Di Sarli, A.R. Color stability in mortars and concretes. Part 1: Study on architectural mortars. Construction and Building Materials. 2016. 120. Pp. 617–622. DOI: 10.1016/j.conbuildmat.2016.05.133
28. López, A., Guzmán, G.A., Di Sarli, A.R. Color stability in mortars and concretes. Part 2: Study on architectural concretes. Construction and Building Materials. 2016. 123. Pp. 248–253. DOI: 10.1016/j.conbuildmat.2016.06.147
29. Bazhenova, O., Kotelnikov, M. Operational features of decorative concrete. E3S Web of Conferences. 2018. Pp. 02021. DOI: 10.1051/e3sconf/20183302021
30. Kopecskó, K. Self-compacting concrete produced with limestone waste. IOP Conference Series: Materials Science and Engineering. 2018. Pp. 012006. DOI: 10.1088/1757-899X/442/1/012006
31. Slavcheva, G.S., Artamonova, O.V. The rheological behavior of disperse systems for 3D printing in constrcution: the problem of control and possibility of «nano» tools application. Nanotechnologies in Construction: A Scientific Internet-Journal. 2018. 10(3). Pp. 107–122. DOI: 10.15828/2075-8545-2018-10-3-107-122
32. Slavcheva, G.S., Artamonova, O. V. Rheological behavior of 3D printable cement paste: Criterial evaluation. Magazine of Civil Engineering. 2018. 84(8). Pp. 97–108. DOI: 10.18720/MCE.84.10

Information about authors:

***Galina Slavcheva**, Sc.D. in Technical Science*
ORCID: https://orcid.org/0000-0001-8800-2657
E-mail: gslavcheva@yandex.ru

Ekaterina Britvina,
ORCID: https://orcid.org/0000-0002-0462-4991
E-mail: esolovieva@vgasu.vrn.ru

Received 24.06.2021. Approved after reviewing 11.11.2021. Accepted 12.12.2021.